Journal of Applied Electrochemistry (2022) 52:189–202
https://doi.org/10.1007/s10800-021-01634-1

RESEARCH ARTICLE

Efficient electrochemical oxidation of reactive dye using a novel Ti/nanoZnO–CuO anode: electrode characterization, modeling, and operational parameters optimization

Nastaran Akbari[1] · Farideh Nabizadeh Chianeh[1] · Ali Arab[1]

Received: 31 May 2021 / Accepted: 25 September 2021 / Published online: 10 October 2021

Abstract

In the current study, electrochemical removal of reactive orange 7 (RO7) dye in aqueous solution was examined over a novel Ti/nanoZnO–CuO electrode prepared through electrophoretic deposition technique. Surface morphology, crystal structure, and elemental investigation of the prepared electrode were done by Field emission scanning electron microscopy, X-ray energy dispersive spectrometry, and X-ray diffraction analysis, which confirmed the presence of CuO nanoparticles along with ZnO nanoparticles in uniform coated layer. Besides, some electrochemical properties of the Ti/nanoZnO–CuO electrode were evaluated applying linear sweep voltammetry, cyclic voltammetry, and electrochemical impedance spectroscopy analysis. Based on these analyses, the Ti/nanoZnO–CuO electrode behaves as a non-active electrode as well as it possessed smaller charge-transfer resistance and higher current density than Ti and Ti/nanoZnO electrodes. Further, chrono-amperometry along with chrono-potentiometry tests were conducted to assess the novel electrode stability and service lifetime. Obtained results indicated the presence of CuO nanoparticles conducive to the enhancement of stability and conductivity properties. To evaluate the prepared electrode performance and optimize the removal process, four independent variables of pH, electrolyte concentration, current, and reaction time as inputs along with RO7 removal efficiency as response function in central composite design were investigated. Under optimal conditions, the RO7 removal efficiency and chemical oxygen demand of 99.16% and 66.66% were obtained after 60 min for Ti/nanoZnO–CuO electrode. According to the obtained results, Ti/nanoZnO–CuO electrode can be used in the electrochemical treatment of organic pollutants as a promising electrode.

✉ Farideh Nabizadeh Chianeh
Nabizadeh@semnan.ac.ir

[1] Department of Chemistry, Semnan University, Semnan, Iran

Graphic abstract

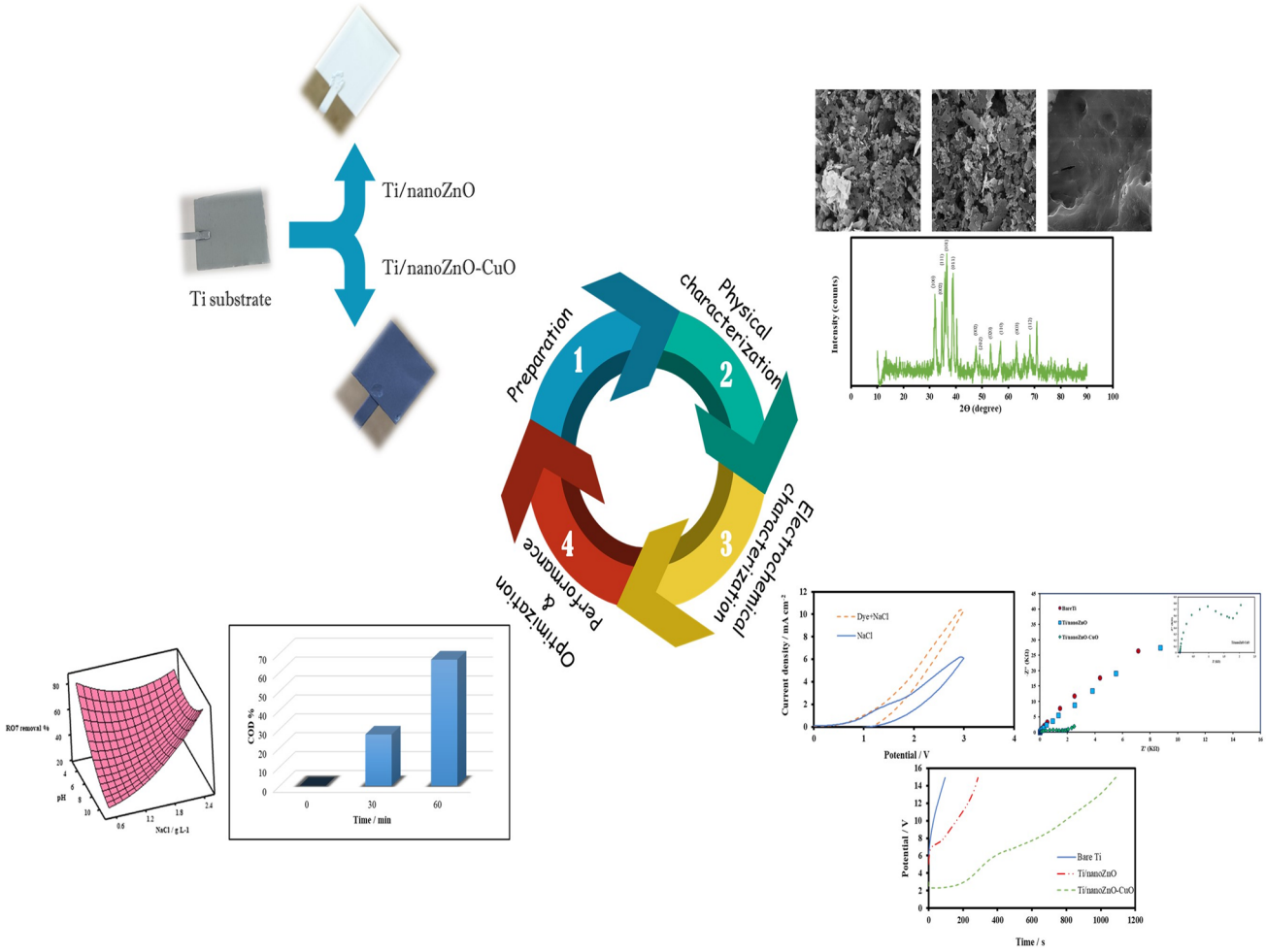

Keywords Electrochemical oxidation · Reactive orange 7 · Ti/nanoZnO–CuO electrode · Modeling

1 Introduction

Over the past decades, along with the developed countries industrialization, a huge amount of contaminated water by various organic pollutants (specifically dyes) have been discharged into the aquatic ecosystem without suitable prior treatment [1, 2] The presence of synthetic organic dyes can cause further problems of these effluents discharging since synthetic dyes are persistent pollutants and might remain in the surface water bodies for a long time. Moreover, the effluent including synthetic dyes are greatly colored which inhibits sunlight penetration, and also some organic dyes can cause mutagenic and carcinogenic problems in humans [3]. Based on the abovementioned problems, it can be said that dyes are complex aromatic compounds with a high level of stability, hence, they are almost resistant to degrade by conventional treatment methods [4, 5]. In the last decades, electrochemical technology has been greatly developed for different wastewater treatment due to its versatility, environmental friendliness, and safety [5, 6]. Among the electrochemical removal methods, the electrochemical advanced oxidation processes (EAOPs) method attracted considerable attention of environmental researchers due to its high degradation and mineralization efficiency, easy operation, and no sludge generation [7]. The EAOPs efficiency depends upon the substrate, and preparation method of the anode, electrolyte concentration, applied current density, as well as pollutant concentration [8, 9]. During the electrochemical oxidation process, among the affecting mentioned parameters the

anode material plays a critical role and remarkably affects the pollutant oxidation efficiency [10]. Therefore, it will be of notable benefit to investigate a novel and suitable electrode material with high electro-catalytic efficiency for the electrochemical removal process. It is worth noting that good anode materials should not only be effective in treatment processes but also cost-effective and stable electrochemically. On the other hand, researchers studying in this field found that the anode surface modification using nanoparticles significantly enhances the active surface area and improves the electrochemical removal rate [11, 12]. So far, various electrodes such as Platinum, Graphite, Boron doped diamond (BDD) electrodes as well as titanium (Ti) based dimensional stable anodes (DSAs) have been employed for the removal of organic pollutants [13]. Furthermore, the results of various studies showed that in the treatment processes by Ti-based DSA electrodes, the Ti is highly reactive and oxidized rapidly, hence, an unstable current is observed during the process. In this regard, different types of Ti-based metal oxide electrodes like TiO_2, IrO_2, ZnO, RuO_2, Al_2O_3, CuO, PbO_2, SnO_2, and AgO have been investigated to study the removal of organic pollutants [14, 15]. Among the above coating nanoparticles, Zinc oxide nanoparticles (ZnO–NPs) are n-type semiconductors with a wide bandgap near 3.3 eV. The ZnO–NPs salient features are wide availability, excellent electrochemical properties, non-toxicity, high physical and chemical stability, the conductivity of 10^{-7}–10^{-3} S cm^{-1}, low cost, and relatively high photocatalytic activity [12, 16, 17]. At the same time, Copper oxide nanoparticles (CuO NPs) as another attractive semiconductor, has become an important option in catalysis processes as advanced materials, chemical sensors, lithium-ion batteries, adsorbent materials, and antimicrobial materials owing to their high optical absorption coefficient, physical and chemical stability, natural p-type conductivity, catalytic and antibacterial properties [16–19]. Despite the large number of published papers describing the application of ZnO–CuO nano-composite, especially as photo-catalysts, to the best of our knowledge, modification of the Ti substrate by a layer of ZnO–CuO nano-composite through electrophoretic deposition (EPD) method has not been reported so far as anode for electrochemical removal of organic pollutants. It can thus be suggested that coating Ti substrate with ZnO–CuO nanocomposite thin film is a promising design of the anodes to achieve a possible synergic effect between ZnO and CuO nanoparticles and the effective electro-catalytic oxidation ability of toxic organic pollutants. Herein, a novel Ti/nanoZnO–CuO composite electrode was fabricated for the first time through a versatile, simple, cost-effective, and efficient EPD technique. Typically, the EPD process consists of two steps, the first of which occurs when the charged particles in a colloidal suspension electrically migrate to the substrate with the opposite charge under the application of an electric field. Following, particles deposit on the substrate surface in the second step and create a highly dense and uniform film [16, 17, 20].

The surface morphology, chemical composition, crystalline structure, and electrochemical properties of the prepared Ti/nanoZnO–CuO electrodes were characterized by means of field emission scanning electronic microscopy (FESEM), energy-dispersive X-ray spectroscopy (EDS), X-ray diffraction (XRD), linear sweep voltammetry (LSV), cyclic voltammetry (CV), electrochemical impedance spectroscopy (EIS), chrono-amperometry (CA), and chrono-potentiometry (CP). The main objective of present study was to assess the electro-catalytic activity of a novel prepared Ti/nanoZnO–CuO electrode as an anode for the electrochemical decolorization of reactive orange 7 (RO7) dye as the target pollutant from aqueous solution. Further, response surface methodology (RSM) using central composite design (CCD) (as a statistical method) was applied to identify the relationship of the factors and response, the interactions among the independent variables, the optimum operational conditions, and the relative significance of the factors in multivariable systems [21, 22]. As a final analysis, chemical oxygen demand (COD) removal was performed to determine RO7 dye mineralization efficiency in an aqueous solution as a function of optimal conditions.

2 Experimental

2.1 Materials

Oxalic acid ($C_2H_2O_4$–$2H_2O$) with 98% purity (Merk) and sodium hydroxide (NaOH) (Merk) were used for cleaning the Ti substrate. ZnO (99.9% purity) and CuO (99% purity) metal oxide nanoparticles were purchased from Neutrino Corporation, Iran, and used for the ZnO and ZnO–CuO nano-composite deposition. N, N Dimethylformamide (DMF) solvent (Carlo, France) and Nickel (II) chloride ($NiCl_2$) (Merk) were used in the EPD coating process. All other chemicals namely sodium chloride (NaCl), sodium sulfate (Na_2SO_4), hydrochloric acid (HCl), and NaOH were obtained from Merck Co. and were used for the electrochemical measurements and the adjusting operational condition for removal experiments. The synthetic RO7 dye (Alvan Sabet Company, Hamedan, Iran) characteristics are given in Table 1S. To prepare a stock solution, a specific amount of RO7 dye in powder form was dissolved into the distilled water and then diluted into a concentration of 50 mg L^{-1} for each experimental run. The stock solution was stored in a dark place for further use after dilutions to prevent

decolorization. All chemicals and reagents used in this work were of analytical grade.

2.2 Preparation of the Ti/nanoZnO–CuO electrode

Prior to the deposition of ZnO–CuO nano-composite film, titanium plates (2 cm × 2 cm × 0.5 mm) were pretreated according to the procedure detailed in our previous study [23]. The ZnO–CuO nano-composite films were electrodeposited on the pretreated Ti substrate by the following steps: Initially, the electrodeposition solution was prepared in a cylindrical Pyrex glass vessel as follows: the ZnO and CuO nanoparticles at a molar ratio of 2:1 and $NiCl_2$ charger salt as an additive (less than 1%) were dispersed uniformly in 50 mL DMF by sonication in an ultrasonic probe for 20 min. Afterward, cathodic EPD was carried out in a uniform suspension at a current of 0.005 A for 2 min using a pretreated Ti plate as the cathode and two other same-size Ti plates served as anodes with a distance of approximately 1 cm. This procedure was subsequently repeated several times until the Ti plate was thoroughly covered by the desired amount of catalytic film. At last, the electrodes were air-dried horizontally at room temperature overnight and then annealed at 350 °C in a furnace for 3 h.

2.3 Physicochemical characterization and electrochemical measurement of Ti/nanoZnO–CuO electrode

The surface morphology of the Ti substrate as well as ZnO–NPs and ZnO–CuO nano-composite coatings were examined by field emission scanning electron microscope (FESEM, TE-SCAN; MIRA3; Czech). The elemental

Table 1 Central composite design array in uncoded units and the value of response function (CR%)

Run order	pH	NaCl	*I*	*T*	Experimental	Predicted
1	7	1.5	0.003	15	11.92	5.39
2	5	1	0.002	30	9.08	12.38
3	3	1.5	0.003	45	72.60	67.43
4	9	2	0.004	60	73.68	74.93
5	5	1	0.004	30	53.39	58.16
6	7	1.5	0.003	45	42.31	43.42
7	9	2	0.004	30	13.92	18.66
8	7	1.5	0.003	45	43.07	43.42
9	5	2	0.002	30	21.63	24.38
10	7	1.5	0.003	75	82.22	82.18
11	7	1.5	0.003	45	46.56	43.42
12	7	1.5	0.005	45	58.70	54.57
13	9	1	0.002	60	29.85	33.56
14	5	2	0.004	30	42.71	43.56
15	5	1	0.004	60	92.77	96.31
16	7	1.5	0.003	45	42.11	43.42
17	7	2.5	0.003	45	70.60	67.76
18	7	1.5	0.003	45	43.33	43.42
19	5	2	0.004	60	93.83	93.94
20	9	1	0.004	60	61.3	60.54
21	5	1	0.002	60	35.64	35.82
22	9	1	0.002	30	5.28	7.16
23	11	1.5	0.003	45	44.60	43.19
24	7	1.5	0.003	45	43.65	43.44
25	7	0.5	0.003	45	45.09	41.36
26	5	2	0.002	60	52.86	53.17
27	7	1.5	0.003	45	43.01	43.42
28	9	2	0.002	60	77.33	74.55
29	7	1.5	0.001	45	10.85	8.41
30	7	1	0.004	30	16.21	16.50
31	7	2	0.002	30	34.91	35.92

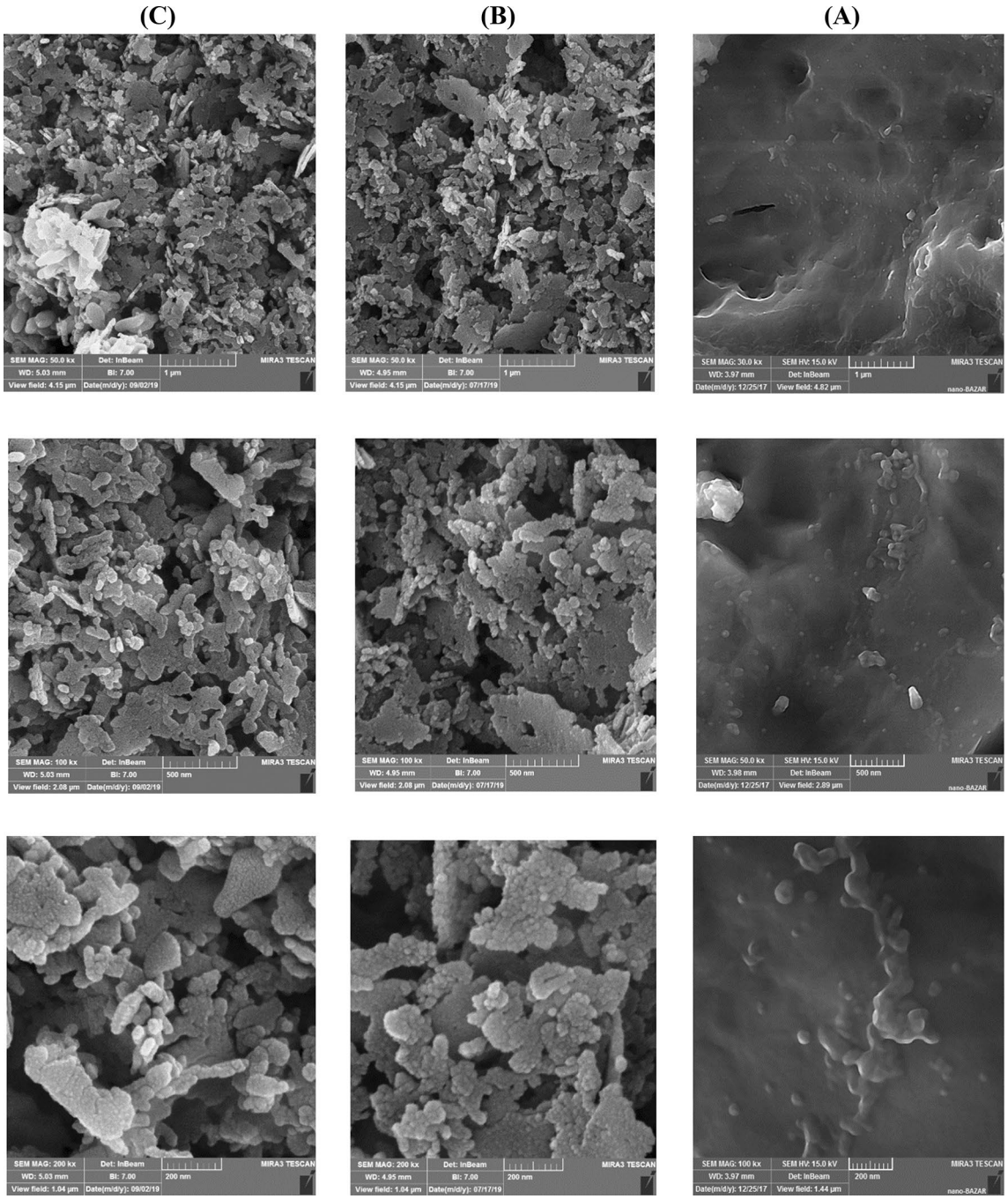

Fig. 1 The FE-SEM images of **A** Bare Ti, **B** Ti/nanoZnO, and **C** Ti/nanoZnO–CuO electrodes

analysis of the Ti/nanoZnO–CuO electrode was observed by energy-dispersive X-ray spectroscopy (EDS, Oxford Instrument; England) attached to FESEM. X-ray diffraction (XRD, D8, Bruker, Germany) patterns were collected using a diffractometer with a Cu Kα X-ray source ($\lambda = 0.15406$ nm) over the range of 20°–80° to analyze the crystalline structure and phase composition of the coated film.

In this study, Ti/ nanoZnO and Ti/nanoZnO–CuO electrodes were characterized electrochemically by LSV, CV, CA, and CP through three-electrode cell system (Origa flex, Origalys, France). Ti and prepared electrodes, a platinum wire, and Ag/AgCl/KCl (sat'd) electrode used as the working, counter, and reference electrodes, respectively. At the same time, the EIS tests were executed through Ivium stat Potentiostat/Galvanostat device model Vertex (Netherland).

The oxidative property of Ti/nanoZnO–CuO electrodes was analyzed by CV measurement in 1 g L^{-1} NaCl solution in the presence and absence of 50 mg L^{-1} RO7 dye with a scan rate of 50 mV s^{-1} between 0 and 3.0 V. All other electrochemical characterization tests were carried out in 0.1 mol L^{-1} Na_2SO_4 aqueous solution. The LSV experiments were carried out at a scan rate of 50 mV s^{-1} to characterize the oxygen evaluation potential (OEP) and chlorine evolution potential (CEP) (in 1 g L^{-1} NaCl solution) responses of the electrodes. The EIS measurements were also taken at an open-circuit potential with a frequency range between 100 kHz and 10 mHz and the obtained results were fitted using Z view software. The CP and CA tests were carried out as a function of time at the anode current density and potential of 50 mA cm^{-2} and 4 V, respectively, to evaluate anode stability.

2.4 Experimental design

The CCD under RSM, which is an efficient optimization tool, was applied to seek the interaction between independent variables and achieve the optimum conditions for the electrochemical removal process. According to this method, a CCD modeling based on four independent variables [pH, current (A), electrolyte concentration (g L^{-1}), and electrolysis time (min)], consisting of 31 experimental runs was taken to model color removal efficiency of RO7 (response) in optimization section. The natural values and coded levels of mentioned factors are listed in Table 2S. The critical ranges of the four independent variables were determined by some preliminary experiments. Table 1 summarizes the data on the experimental conditions (in the form of the uncoded unit) by CCD along with the actual and predicted responses for dye removal. The color removal efficiency [CR (%)] was calculated according to the UV–Vis data through Eq. (1):

$$RO7\% = \frac{(A_0 - A_t)}{A_0} \times 100, \quad (1)$$

where A_0 and A_t are the absorbance before and after the decolorization process, respectively.

The color removal efficiency data were then analyzed and interpreted applying analysis of variance (ANOVA) (e.g., R^2, adjusted R^2, *t*-test, and *F*-test), and response plots using Minitab 16 software. Following this, a second-order quadratic polynomial equation was resulted to give an explanation for the interaction between the independent variables and the dependent response in the removal process.

3 Results and discussion

3.1 Morphological and structural characterization of Ti/nanoZnO–CuO electrode

Figure 1 depicts the surface morphology FE-SEM images of (A) Ti, (B) Ti/nanoZnO, and (C) Ti/nanoZnO–CuO electrodes at different (1 µm, 500 nm, and 200 nm) magnifications. As shown in Fig. 1A, the oxalic acid-etched titanium surface is relatively rough which is expected to strengthen the adhesion and interaction of the coating layer and substrate [24]. As indicated in Fig. 1B along with (C), FE-SEM images of Ti/nanoZnO and Ti/nanoZnO–CuO electrodes, ZnO nanoparticles and ZnO–CuO nanocomposite successfully coated the Ti substrate surface which led to more porous and rougher structures than Ti substrate. On the other hand, in Fig. 1B, the Ti surface modified with ZnO–NPs has pores that improve electrochemical activity. Further, Fig. 1C showed the uniform distribution of CuO–NPs in ZnO–NPs which CuO–NPs easily filled the ZnO pores due to the small size of CuO–NPs; this phenomenon was resulted

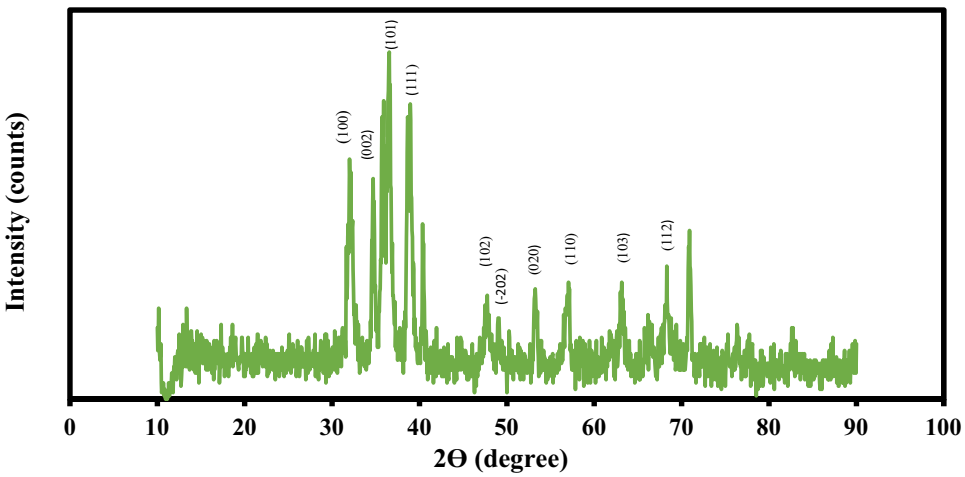

Fig. 2 The XRD pattern of Ti/nanoZnO–CuO electrode

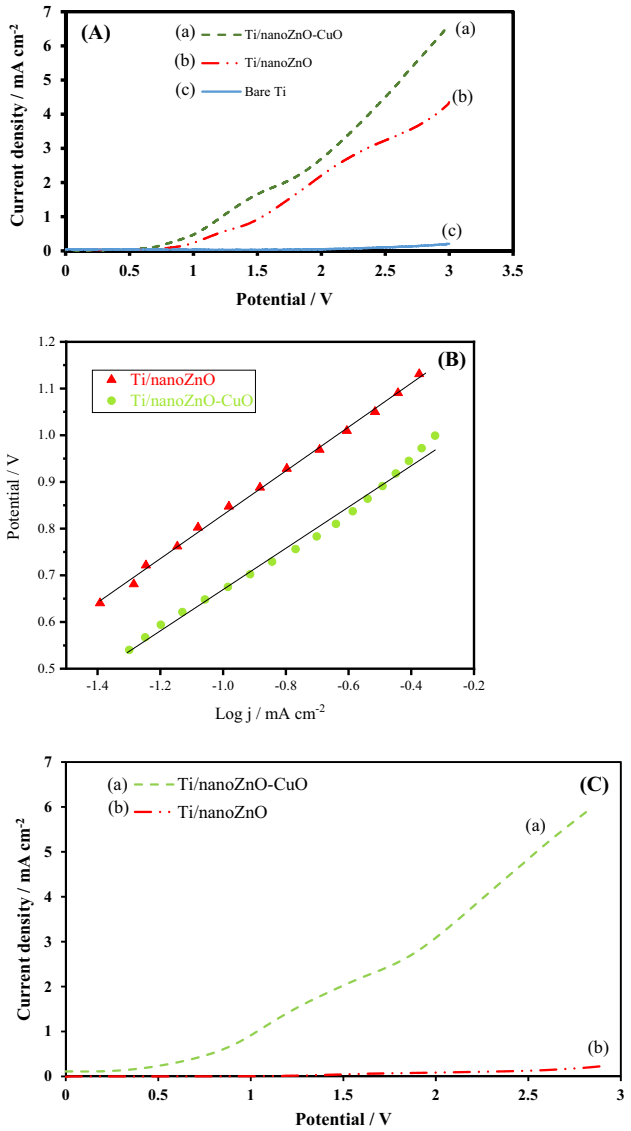

Fig. 3 **A** Linear sweep voltammetry curves of Bare Ti, Ti/nanoZnO, and Ti/nanoZnO–CuO electrodes in 0.1 mol L^{-1} Na_2SO_4 solution at scan rates of 50 mV s^{-1}, **B** Tofel plots of Ti/nanoZnO–CuO and Ti/nanoZnO, **C** Linear sweep voltammetry curves of Ti/nanoZnO and Ti/nanoZnO–CuO in 1 g L^{-1} NaCl solution at scan rates of 50 mV s^{-1}

in creating a more uniform and dense surface [25, 26]. Therefore, according to the surface morphology of the Ti/nanoZnO–CuO electrode compared to Ti/nanoZnO and even Ti electrodes, since the electrocatalytic reactions happen on the surface of electrodes, this expected that the prepared Ti/nanoZnO–CuO electrode exhibits better performance in the electrochemical removal of organics. Subsequent analyses in this study were also performed to further confirm the presence of CuO nanoparticles.

In order to measure the chemical composition along with confirmation of components in the ZnO–CuO nanocomposite coated layer, an EDS analysis was performed. Figure 1S shows the EDS spectrum of Ti/nanoZnO–CuO electrode, which verifies the presence of Zn, O, Cu, and Ti [17, 27]. In addition to EDS, XRD pattern is also utilized to further examine the elemental composition of the ZnO–CuO nano-composite. From Fig. 2, the diffraction peaks locating at $2\theta = 32.03°$, 34.70°, 36.53°, 47.78°, 57.10°, 63.12°, and 68.30° were ascribed to the (100), (002), (101), (102), (110), (103), and (112) planes of the ZnO–NPs, while (002), (111), (− 202) and (020) planes at $2\theta = 35.80°$, 38.79°, 49.04°, and 53.24° were assigned to CuO–NPs [28]. Furthermore, all the diffraction peaks of the ZnO–CuO nano-composite in Fig. 2 show no diffraction peaks of impurities and crystallized TiO_2 (the result of Ti substrate oxidation). Besides, the crystallite size values were estimated using the Debye–Scherrer's equation, the result was stated in Table 3S.

3.2 Electrochemical characterization of Ti/nanoZnO–CuO electrode

In order to probe the impact of CuO–ZnO nano-composite and ZnO–NPs coating, LSV analysis was used to probe the oxygen evolution potentials (OEP) of the Ti/nanoZnO–CuO and Ti/nanoZnO electrodes (Fig. 3A) [29]. From this figure, it can be clearly seen the reduction in overpotential value of the Ti/nanoZnO–CuO and Ti/nanoZnO electrodes compared to conventional Ti electrode which might be related to enhanced active sites for reactions of oxygen evolution on prepared electrodes [30, 31]. Furthermore, the presence of CuO–NPs in the ZnO–CuO nano-composite has played a significant role in improving the oxygen evolution current density. Therefore, the mentioned enhancement leads to higher electrocatalytic activity in the oxidation of organic pollutants through Ti/nanoZnO–CuO electrode than Ti/nanoZnO electrode [32]. Tafel graph was drawn from LSV data (Fig. 3B) for further electrochemical investigation on the Ti/nanoZnO–CuO electrode. According to the obtained result, in a linear fitting of Tafel data for two electrodes using Origin software, the Ti/nanoZnO–CuO electrode (0.44 V dec^{-1}) showed a lower slope compared to Ti/nanoZnO electrode (0.46 V dec^{-1}), which led to better electrocatalytic activity [33, 34]. Furthermore, according to the Fig. 3C, it can be clearly seen that introduction of CuO–NPs resulted in a decrease in CEP value for Ti/nanoZnO–CuO electrodes, suggesting that chlorine species can be formed more easily. In this regard, the presence of produced active chlorine species can have a role in the electrochemical removal (mainly decolorization) of dyes [35, 36]. Comparison of OEP and CEP values can provide evidence of earlier evolution of the active chlorine species than side reaction for oxygen evolution. Due to this, active chlorine species can have contributions to electrochemical oxidize pollutants by electrochemical methods via Ti/nanoZnO–CuO electrode in removal processes [24].

Cyclic voltammograms of Ti/nanoZnO–CuO electrode (0.5×0.5 cm^2) in the 1 g L^{-1} NaCl solution with and without the 50 mg L^{-1} of RO7 at a scan rate of 50 mV s^{-1} in the potential range between 0.0 V and 3.0 V are displayed in Fig. 4. As can be seen in this figure, when RO7 was added into the NaCl electrolyte, no additional oxidation peak was observed, which showed that the Ti/nanoZnO–CuO electrode does not participate in the direct electrochemical oxidation reaction of RO7 dye and behaves as a non-active electrode [32, 37]. Thus, it could be concluded that RO7 electro catalytic removal was achieved via hydroxyl radicals together with other oxidant species.

Further, for the sake of monitoring the electrochemical effect of the CuO–ZnO nano-composite and ZnO–NPs coated layers on the Ti substrate based on the EPD coating method, EIS analysis, as a well-known technique, was employed to study interfacial characteristics of the coated layer. Figure 5 presents the resultant Nyquist plots and equivalent circuit for the Ti, Ti/nanoZnO, and Ti/nanoZnO–CuO electrodes in a three-electrode system at frequencies swept from 100 kHz to 0.01 Hz in 0.1 mol L^{-1} Na_2SO_4 at an open-circuit potential [38, 39]. In general, each Nyquist plot consists of two parts: a semicircle arc part at the high-frequency range and a linear part at the low-frequency range which corresponds to the charge-transfer process and the radius attributed to the electrolyte diffusion, respectively. It can be clearly observed that the Ti/nanoZnO–CuO electrode has the smallest arc diameter, which reveals that the introduction of CuO–NPs considerably reduced the charge-transfer resistance of the modified electrode compared with bare Ti and Ti/nanoZnO electrodes. Moreover, the fitted

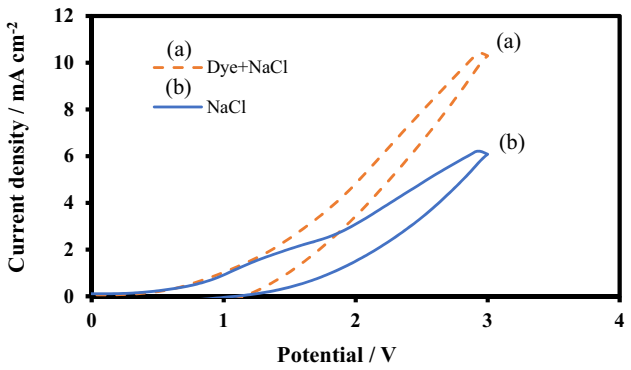

Fig. 4 Cyclic voltammograms of Ti/nanoZnO–CuO in absence and presence of 50 mg L^{-1} RO7 at 50 mV s^{-1} scanning rate

parameters (Rs, Rct, and CPE) of the equivalent circuit models are listed in Table 4S. In Rs [Rct CPEdl] equivalent circuit for bare Ti and Ti/nanoZnO electrodes, Rs and Rct represent the solution resistance and charge transfer, while CPEdl is associated with constant phase element of double layer. Besides, additional parameter (CPE0) in Rs [CPEdl (RctCPE0)] equivalent circuit is constant phase element. On the basis of obtained Rct values, the modified electrode possessed the smallest Rct, which indicates the improvement of conductivity and electrocatalytic activity [32, 39].

Since the stability of electrode is important in practical applications of the electrochemical oxidation process, CA tests were conducted to evaluate the stability of Ti, Ti/nanoZnO, and Ti/nanoZnO–CuO electrodes with the dimension of 2×2 cm^2 in a solution of 0.1 mol L^{-1} Na_2SO_4 at 4 V during the 1800s. According to CA responses in Fig. 6, it can be said that Ti/nanoZnO–CuO electrode indicated a higher current response rather than other electrodes throughout the test under the same conditions [40–42]. As indicated shown in Fig. 6, the Ti electrode shows a low current density, and also this parameter has a sharp current decrease near to zero in the initial few seconds because of the Ti surface deactivation. Besides, the current density of Ti/nanoZnO declines but almost near to 4V [43–48]. In comparison to these electrodes, the Ti/nanoZnO–CuO electrode provides better current density value and stability which indicates a slower deactivation of this electrode. In addition, the high current density in the CA response of Ti/nanoZnO–CuO electrode could be attributed to more active sites resulted from CuO–NPs presence. Therefore, obtained results confirm the superior electrochemical performance of the Ti/nanoZnO–CuO over Ti and Ti/nanoZnO electrodes [40, 49].

An important factor in the evaluation of electrode quality is its service lifetime as well as its electrochemical stability, which affected by various parameters such as current density, temperature, and pH of the electrolyte. Therefore, the CP analysis was carried out to further assess the stabilities of Ti/nanoZnO–CuO, Ti/nanoZnO, and Ti electrodes. The CP diagrams were recorded with a constant current density of 50 mA cm^{-2} were indicated in Fig. 7. It is worth noting that, regarding the difficulty of evaluating the actual service life of electrodes at low current density values due to the relatively long process; the following empirical relationship can help to assess the actual lifetime of the electrodes in different current densities.

$$\Gamma 2 = \left(\frac{i_1}{i_2}\right)^2 \Gamma 1, \tag{2}$$

where Ţ1 and Ţ2 are accelerated and actual service life, respectively, as well as i_1 and i_2 are accelerated and actual current density, respectively. According to the results shown in Fig. 6, the accelerated lifetime of the Ti/nanoZnO–CuO electrode (963.3 s) under accelerated test conditions is 3.4 times longer than that of the Ti/nanoZnO electrode (283 s). The calculated actual service life of Ti/nanoZnO–CuO, Ti/nanoZnO, and Ti electrodes in 5 mA cm^{-2} was 26.76, 7.5,

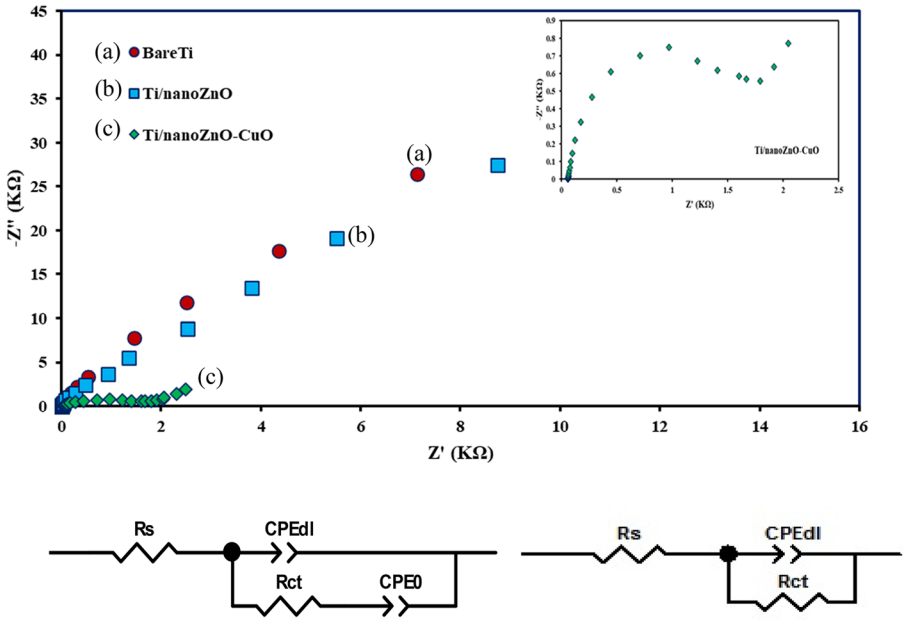

Fig. 5 Nyquist plots of Bare Ti, Ti/nanoZnO, and Ti/nanoZnO–CuO electrodes and fitted equivalent circuit of **A** Bare Ti and Ti/nanoZnO, **B** Ti/nanoZnO–CuO in 0.1 mol L^{-1} Na_2SO_4 solution at open-circuit potential

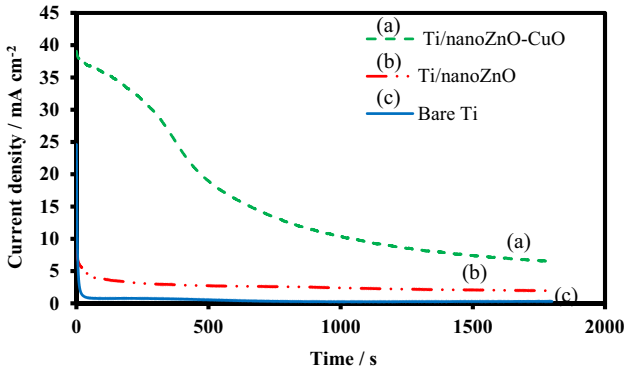

Fig. 6 Chrono-amperograms of Bare Ti, Ti/nanoZnO, and Ti/nanoZnO–CuO electrodes for 30 min

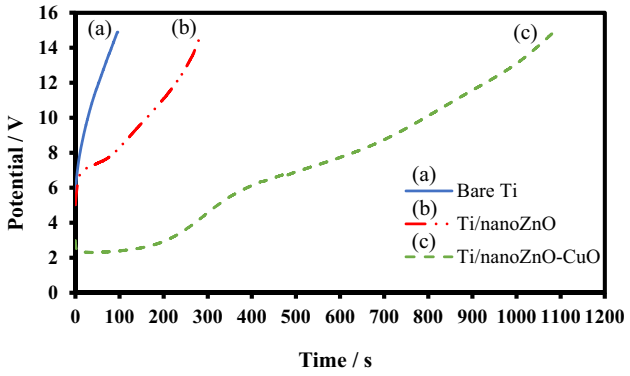

Fig. 7 Chrono-potentiometry curves of Bare Ti, Ti/nanoZnO, and Ti/nanoZnO–CuO electrodes in 0.1 mol L^{-1} Na_2SO_4 solution

and 2.56 h, respectively. It is worth pointing out, the longer actual service life of coated electrodes than Ti electrode can be attributed to the deposition of coating layers on the surface of the Ti substrate, which prevents the phenomenon of passivation. On the other hand, the introduction of CuO–NPs leads to enhancement in conductivity as well as actual service life than Ti/nanoZnO [41, 42, 48].

3.3 Optimization of operational parameters in RO7 electrochemical removal

As stated in Sect. 2.4, a second-order quadratic polynomial equation was proposed for RO7 removal efficiency which x_i (x_j), β_0, β_i, and β_{ij} are design independent variables, a constant coefficient, *i*th linear coefficient, and *ij*th interaction coefficient, respectively [43, 45]. The general form and proposed quadratic equations are:

$$Y = \beta_0 + \sum \beta_i X_i + \sum \beta_{ii} X_i^2 + \sum \beta_{ij} X_i X_j + \varepsilon, \quad (3)$$

$$\begin{aligned} Y = {} & \beta_0 + \beta_1 x_1 + \beta_2 x_2 + \beta_3 x_3 + \beta_4 x_4 + \beta_{11} x_1^2 \\ & + \beta_{22} x_2^2 + \beta_{33} x_3^2 + \beta_{44} x_4^2 + \beta_{12} x_1 x_2 + \beta_{13} x_1 x_3 \\ & + \beta_{14} x_1 x_4 + \beta_{23} x_2 x_3 + \beta_{24} x_2 x_4 + \beta_{34} x_3 x_4, \end{aligned} \quad (4)$$

$$\begin{aligned} Y = {} & -40.8 - 8.26\, x_1 - 28.0\, x_2 + 68045\, x_3 - 0.593\, x_4 \\ & + 0.743\, x_1^2 + 11.13\, x_2^2 - 2983914\, x_3^2 + 0.00040\, x_4^2 \\ & + 4.19\, x_1 x_2 - 4555\, x_1 x_3 + 0.0491\, x_1 x_4 - 13301\, x_2 x_3 \\ & + 0.408\, x_2 x_4 + 294.0\, x_3 x_4. \end{aligned} \quad (5)$$

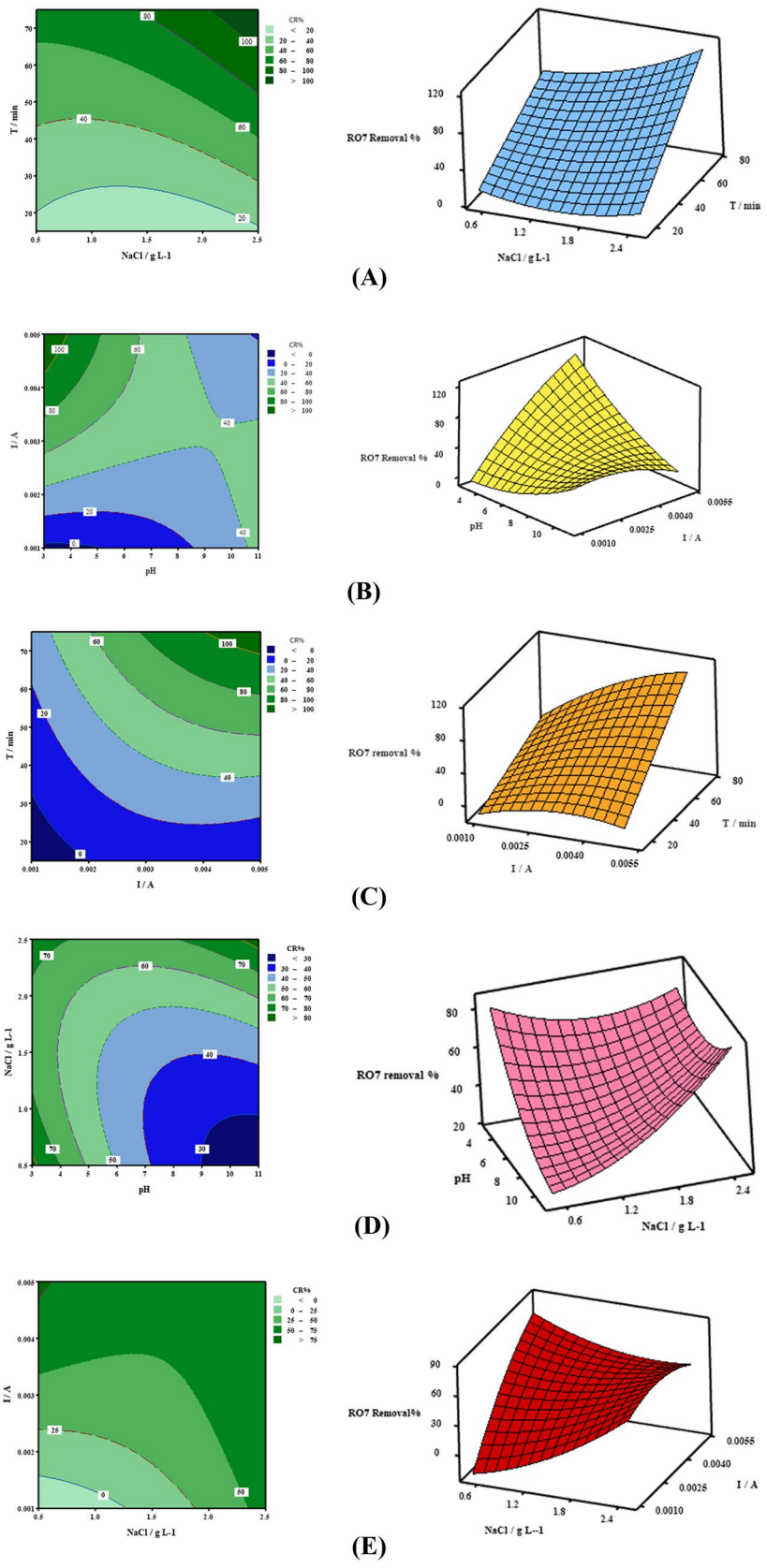

Fig. 8 Response surface and counter plots showing the effects of **A** pH—current, **B** electrolyte concentration—reaction time, **C** current—reaction time, **D** electrolyte concentration—pH, and **E** electrolyte concentration—current on color removal efficiency (CR%)

The adequacy of mathematical models and suitability of the response function resulting from CCD was studied by analysis of variance (ANOVA), the data is listed in Table 5S. The terms with the p value smaller than 0.05 (with a 95% confidence level) are more significant, hence, other terms can be omitted. Besides, according to Table 5S, most of the terms are significant, so it can be concluded that the predicted model is appropriate [46, 47]. On the other hand, the proposed model for the RO7 electrochemical removal is in good correlation ($R^2 = 0.9854\%$) showed that 98.54% of data could be explained by the regression model, while neglect number of data could not be explained. Also, Student's t-test along with p value investigation were used to determine the significance of the terms in the proposed model. Table 6S presented the student's distribution and the corresponding values for the proposed model for RO7 electrochemical removal by Ti/nanoZnO–CuO [44, 50]. As mentioned above, the insignificant terms can be omitted, which resulted in Eq. 6 [51].

$$\begin{aligned} Y = & -40.8 - 8.26x_1 - 28.0\,x_2 + 68045\,x_3 - 0.593\,x_4 \\ & + 0.743\,x_1^2 + 11.13\,x_2^2 - 2983914\,x_3^2 + 0.00040\,x_4^2 \\ & + 4.19\,x_1x_2 - 4555\,x_1x_3 + 0.0491\,x_1x_4 - 13301\,x_2x_3. \end{aligned} \tag{6}$$

The residuals plot (the difference between the experimental and the predicted responses) as additional tools were employed to evaluate the proposed model adequacy. As illustrated in Fig. 2S, the points in the normal probability plot are indicated a straight line which shows the good normally distribution of data in the proposed model [52].

Pareto analysis as a bar graph can be performed to give more information to interpret obtained results. In fact, this analysis determines the impact of each parameter (percent) on the response (Eq. 7) [53].

$$P_{\mathrm{i}} = \frac{b_{\mathrm{i}}^2}{\sum_{i=1}^{n} b_{\mathrm{i}}^2}. \tag{7}$$

According to Fig. 3S, it can be seen that factors reaction time ($\beta_4 = 48\%$), current ($\beta_3 = 28\%$), and pH-current interaction ($\beta_{13} = 12\%$) have the most influence on the RO7 removal process.

3.4 Effect of operational parameters on electrochemical removal of RO7

In this section, 3D response Surface and 2D counter plots of interaction between two effective parameters on the response (RO7 removal efficiency) using Ti/nanoZnO–CuO electrode are examined. Based on the ANOVA results, parameters interaction including pH—current, electrolyte concentration—reaction time, current—reaction time, pH—electrolyte concentration, and electrolyte concentration—current were significant terms for the model of RO7 electrochemical removal.

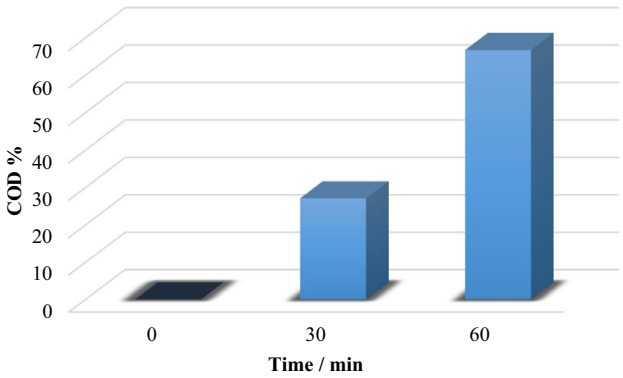

Fig. 9 COD% of color removal efficiency under optimum condition

The interaction relationship between electrolyte concentration and reaction time on the RO7 removal efficiency depicted in Fig. 8A. As the plots imply, using NaCl as an electrolyte can promote reactive species production during the electrochemical oxidation process, which resulted in the achievement of better dye removal efficiency with the passage of the reaction time. The presence of NaCl in undivided cells in the electrochemical oxidation process resulted in producing chlorine (Eq. 8) at the anode as well as producing other chlorine species based on Eqs. (8)–(11). Therefore, it can be said that various chloride species namely Cl_2, Cl_3^-, HClO, and ClO^- are involved in the removal of dye molecules [2, 24, 54] On the other hand, enhancement in the NaCl concentration can improve the solution conductivity as well as ease electron transfer, thereby energy consumption is decreased which is related to the cell voltage [55, 56]. From Fig. 8A, more production of active chlorine species with high decolorizing potential by increasing electrolyte concentration along with reaction time improved the RO7 removal efficiency [57].

$$2Cl^- \rightarrow Cl_{2(aq)} + 2e^-, \tag{8}$$

$$Cl_{2(aq)} + Cl^- \leftrightarrow Cl_3^-, \tag{9}$$

$$Cl_{2\,(aq)} + H_2O \rightarrow H^+ + Cl^- + HOCl, \tag{10}$$

$$HOCl \leftrightarrow H^+ + OCl^-. \tag{11}$$

Figure 8B presents the interaction relationship between pH and current in constant values of reaction time (45 min) and electrolyte concentration (1.5 g L^{-1}). As can be seen in Fig. 8B, reduction in the pH values at all applied current

can led to a significant increase in RO7 removal efficiency. In order to explain the observed trend, the electro-generated oxidizing agents such as hydroxyl radicals and chlorine species can have effects on electrochemical oxidation efficiency. Furthermore, the oxygen evolution side reactions are also a possible explanation for the above tendency [24]. Indeed, the acidic environment condition in these types of removal processes (electrochemical oxidation) could reduce the side reaction of oxygen evolution through the OEP enhancement and promotion of hydroxyl radical formation, which in turn result in improving dye removal efficiency [49, 58]. Further, hypochlorous acid (HClO) as the powerful oxidizing agent in acidic conditions (in the presence of the NaCl supporting electrolyte) has greater oxidation capability compared to hypochlorite, which resulting higher dye removal efficiency. As is also clear from Fig. 8B, the dye removal efficiency was improved by increasing current density. Further details about this observation can be found in the following paragraphs.

Figure 8C illustrates the interaction between the current and the reaction time parameters. According to Fig. 8C, with increasing current together with reaction time, improvement is seen in dye removal efficiency. This phenomenon could be attributed to the production of more reactive species including active chlorine species and hydroxyl radicals with increasing of reaction time [44, 52, 53]. It is worth to note that increasing electron speed and providing more hydroxyl radicals are happen with a rise in the current in this removal process [44].

Electrolyte concentration—pH interaction is another significant term in the RO7 removal process is shown in Fig. 8D. It is worth noting that strong oxidants such as Cl_2, HOCl, and ClO– due to the presence of NaCl electrolyte are beneficial for oxidation progress [59]. Besides, more hydroxyl radicals are expected to be generated through water oxidation at alkaline pH [60, 61]. Therefore, the outcomes demonstrated that these two parameters have a synergistic effect on the response function and enhance the dye removal efficiency by increasing the NaCl electrolyte concentration through various oxidant agents in all pH values.

The interaction of electrolyte concentration and current parameters is shown in Fig. 8E. As shown in this figure, enhancement in current value and NaCl electrolyte concentration increases the RO7 removal efficiency. On the one hand, increasing the current value is conducive to the facilitation of electron transfer along with the production of more reactive species. On the other hand, with raise in NaCl electrolyte concentration, the number of active chlorine species with good potential in decolorization increases, demonstrating that both parameters have a synergetic effect on RO7 removal efficiency [44, 62, 63].

3.5 Validation of the model

The selection of the best operative conditions in the RO7 electrochemical removal process on Ti/nanoZnO–CuO is the main purpose of using experimental design. In this regard, as a validation process of the optimization results, a confirmation experiment was conducted under the predicted optimal conditions. According to Fig. 9, obtained CCD model predicted 96.31% of RO7 removal efficiency at the optimized conditions of 5, 1 g L^{-1}, 0.004 A, and 60 min for pH, electrolyte concentration, current, and reaction time, respectively. The RO7 removal efficiency reached 99.16% in 60 min under the optimal conditions which were closely agreed with the predicted value [64]. Under optimal conditions, after 60 min of electrochemical treatment of RO7 (with the initial concentration of 50 mg L^{-1}) using Ti/nanoZnO–CuO anode, more than 60% of COD removal efficiency was obtained. Comparing the removal efficiencies of color and COD, the lower COD percent is clearly evident due to the decomposition of RO7 molecules into colorless intermediate products which are less reactive to hydroxyl radicals [55, 65]. It is worthwhile mentioning that the COD analysis was performed using HACH Model 3900 DR (Fig. 9).

4 Conclusion

In the present research work, a novel Ti/nanoZnO–CuO composite electrode was prepared through the EPD method which was characterized by different analyses. The SEM analysis revealed that the prepared electrode surface was uniformly coated by ZnO–CuO nano-composite. The presence of ZnO and CuO nanoparticles on the electrode surface was confirmed by obtained results of EDS and XRD analyses. The absence of an additional peak in the CV diagram showed that the Ti/nanoZnO–CuO is a non-active anode and direct electron transfer did not occur between the prepared novel electrode and RO7. Based on the observed data of EIS analysis, the Ti/nanoZnO–CuO electrode had a smaller semicircle diameter (lower electron transfer resistance) than the Ti electrode which is due to the good conductivity and high electron transfer efficiency of CuO nanoparticles. In addition, ZnO–CuO nano-composite coating effectively enhanced the prepared electrode durability and service lifetime compared to conventional Ti and Ti/nanoZnO electrodes as illustrated in CA and CP analyses. Further, the CCD design method under RSM was applied to investigate the effect of four key operating factors on RO7 electrochemical removal efficiency along with optimization of operational conditions. Under optimal conditions, the color and COD removal efficiency of RO7 on Ti/nanoZnO–CuO were 99.16% and 66.66%, respectively. It is worthwhile mentioning that observed electrochemical removal efficiency and

CCD predicted results had high closeness. Ultimately, considering all the results above, the current study provides an efficient novel electrode to use in the electrochemical treatment field. However, further work and more investigation are still required to improve the stability of the prepared electrode and to evaluate the amount of generated oxidants, including the active chlorine species, as well as an in-depth investigation of the degradation mechanism of RO7 during the electrochemical oxidation process through the Ti/nanoZnO–CuO anode.

Supplementary Information The online version contains supplementary material available at https://doi.org/10.1007/s10800-021-01634-1.

Acknowledgements The authors thank the Semnan University, Iran for financial and other supports.

References

1. Ansari A, Nematollahi D (2018) A comprehensive study on the electrocatalytic degradation, electrochemical behavior and degradation mechanism of malachite green using electrodeposited nanostructured β-PbO_2 electrodes. Water Res 144:462–473
2. Brillas E, Martínez-Huitle CA (2015) Decontamination of wastewaters containing synthetic organic dyes by electrochemical methods. An updated review. Appl Catal B 166:603–643
3. Aquino JM, Rocha-Filho RC, Ruotolo LA, Bocchi N, Biaggio SR (2014) Electrochemical degradation of a real textile wastewater using β-PbO_2 and DSA® anodes. Chem Eng J 251:138–145
4. Dhote J, Ingole S, Chavhan A (2012) Review on waste water treatment technologies. Int J Eng Res Technol 1:1–10
5. Martínez-Huitle CA, Brillas E (2009) Decontamination of wastewaters containing synthetic organic dyes by electrochemical methods: a general review. Appl Catal B 87(3–4):105–145
6. Chianeh FN, Parsa JB (2015) Degradation of azo dye in aqueous solution using Ti anode coated with MWCNTs–TiO_2. J Iran Chem Soc 12(1):175–182
7. Ganiyu SO, Martinez-Hutile CA, Oturan MA (2020) Electrochemical advanced oxidation processes for wastewater treatment: advances in formation and detection of reactive species and mechanisms. Curr Opin Electrochem 27:100678
8. Berenguer R, Sieben JM, Quijada C, Morallón E (2016) Electrocatalytic degradation of phenol on Pt-and Ru-doped Ti/SnO_2–Sb anodes in an alkaline medium. Appl Catal B 199:394–404
9. Wang Y, Shen C, Zhang M, Zhang B-T, Yu Y-G (2016) The electrochemical degradation of ciprofloxacin using a SnO_2–Sb/Ti anode: influencing factors, reaction pathways and energy demand. Chem Eng J 296:79–89
10. Hu Z, Cai J, Song G, Tian Y, Zhou M (2020) Anodic oxidation of organic pollutants: anode fabrication, process hybrid and environmental applications. Curr Opin Electrochem 26:100659
11. Kim SP, Choi MY, Choi HC (2016) Photocatalytic activity of SnO_2 nanoparticles in methylene blue degradation. Mater Res Bull 74:85–89
12. Wu W, Huang Z-H, Hu Z-T, He C, Lim T-T (2017) High performance duplex-structured SnO_2–Sb–CNT composite anode for bisphenol A removal. Sep Purif Technol 179:25–35
13. Salazar-Banda GR, Santos GDOS, Gonzaga IMD, Dória AR, Eguiluz KIB (2020) Developments in electrode materials for wastewater treatment. Curr Opin Electrochem 26:100663
14. Dai Q, Zhou J, Weng M, Luo X, Feng D, Chen J (2016) Electrochemical oxidation metronidazole with Co modified PbO_2 electrode: degradation and mechanism. Sep Purif Technol 166:109–116
15. Wang C, Yin L, Xu Z, Niu J, Hou L-A (2017) Electrochemical degradation of enrofloxacin by lead dioxide anode: kinetics, mechanism and toxicity evaluation. Chem Eng J 326:911–920
16. Chen X, Huang Y, Zhang X, Li C, Chen J, Wang K (2015) Graphene supported ZnO/CuO flowers composites as anode materials for lithium ion batteries. Mater Lett 152:181–184
17. Das S, Srivastava VC (2017) Synthesis and characterization of ZnO/CuO nanocomposite by electrochemical method. Mater Sci Semicond Process 57:173–177
18. Chauhan M, Sharma B, Kumar R, Chaudhary GR, Hassan AA, Kumar S (2019) Green synthesis of CuO nanomaterials and their proficient use for organic waste removal and antimicrobial application. Environ Res 168:85–95
19. Raul PK, Senapati S, Sahoo AK, Umlong IM, Devi RR, Thakur AJ, Veer V (2014) CuO nanorods: a potential and efficient adsorbent in water purification. RSC Adv 4(76):40580–40587
20. Nabizadeh Chianeh F, Basiri Parsa J (2016) Decolorization of azo dye CI Acid Red 33 from aqueous solutions by anodic oxidation on MWCNTs/Ti electrodes. Desalin Water Treat 57(43):20574–20581
21. Song Q, Li M, Wang L, Ma X, Liu F, Liu X (2019) Mechanism and optimization of electrochemical system for simultaneous removal of nitrate and ammonia. J Hazard Mater 363:119–126
22. Vepsäläinen M, Ghiasvand M, Selin J, Pienimaa J, Repo E, Pulliainen M, Sillanpää M (2009) Investigations of the effects of temperature and initial sample pH on natural organic matter (NOM) removal with electrocoagulation using response surface method (RSM). Sep Purif Technol 69(3):255–261
23. Mahmoudian F, Chianeh FN, Sajjadi SM (2021) Simultaneous electrochemical decolorization of Acid Red 33, Reactive Orange 7, Acid Yellow 3 and Malachite Green dyes by electrophoretically prepared Ti/nanoZnO–MWCNTs anode: experimental design. J Electroanal Chem 884:115066
24. Abdoulyousefi FM, Chianeh FN, Asghari A (2020) Application of a novel Ti/nanoSnO_2-α-Fe_2O_3 anode for the electro-catalytic degradation of dye pollutant: optimization of operational parameters by central composite design. J Electrochem Soc 167(10):103507
25. Yue H, Xue L, Chen F (2017) Efficiently electrochemical removal of nitrite contamination with stable RuO_2–TiO_2/Ti electrodes. Appl Catal B 206:683–691
26. Zhang C, Tang J, Peng C, Jin M (2016) Degradation of perfluorinated compounds in wastewater treatment plant effluents by electrochemical oxidation with Nano-ZnO coated electrodes. J Mol Liq 221:1145–1150
27. An SJ, Zhu Y, Lee SH, Stoller MD, Emilsson T, Park S, Velamakanni A, An J, Ruoff RS (2010) Thin film fabrication and simultaneous anodic reduction of deposited graphene oxide platelets by electrophoretic deposition. J Phys Chem Lett 1(8):1259–1263
28. Renuka L, Anantharaju K, Vidya Y, Nagaswarupa H, Prashantha S, Nagabhushana H (2017) Synthesis of sunlight driven ZnO/CuO nanocomposite: characterization, optical, electrochemical and photocatalytic studies. Mater Today Proc 4(11):11782–11790
29. Li L, Huang Z, Fan X, Zhang Z, Dou R, Wen S, Chen Y, Chen Y, Hu Y (2017) Preparation and characterization of a Pd modified Ti/SnO_2–Sb anode and its electrochemical degradation of Ni-EDTA. Electrochim Acta 231:354–362
30. Duan X, Sui X, Wang W, Bai W, Chang L (2019) Fabrication of PbO_2/SnO_2 composite anode for electrochemical degradation of 3-chlorophenol in aqueous solution. Appl Surf Sci 494:211–222
31. Wang X, Zhou Y, Tuo Y, Lin Y, Yan Y, Chen C, Li Y, Zhang J (2019) Synthesis and identifying the active site of Cu_2Se@ CoSe

nano-composite for enhanced electrocatalytic oxygen evolution. Electrochim Acta 320:134589
32. Yang Y, Cui L, Li M, Yao Y (2019) Electrochemical removal of metribuzin in aqueous solution by a novel PbO_2/WO_3 composite anode: characterization, influencing parameters and degradation pathways. J Taiwan Inst Chem Eng 102:170–181
33. Aromaa J, Forsén O (2006) Evaluation of the electrochemical activity of a Ti–RuO_2–TiO_2 permanent anode. Electrochim Acta 51(27):6104–6110
34. Chen A, Xia S, Pan H, Xi J, Qin H, Lu H, Ji Z (2018) A promising Ti/SnO_2 anodes modified by Nb/Sb co-doping. J Electroanal Chem 824:169–174
35. Rani BJ, Kumar MP, Ravi G, Ravichandran S, Guduru RK, Yuvakkumar R (2019) Electrochemical and photoelectrochemical water oxidation of solvothermally synthesized Zr-doped α-Fe_2O_3 nanostructures. Appl Surf Sci 471:733–744
36. Tu X, Xiao S, Song Y, Zhang D, Zeng P (2015) Treatment of simulated berberine wastewater by electrochemical process with Pt/Ti anode. Environ Earth Sci 73(9):4957–4966
37. Fajardo AS, Martins RC, Silva DR, Quinta-Ferreira RM, Martinez-Huitle CA (2017) Electrochemical abatement of amaranth dye solutions using individual or an assembling of flow cells with Ti/Pt and Ti/Pt–SnSb anodes. Sep Purif Technol 179:194–203
38. Alver Ü, Tanrıverdi A, Akgül Ö (2016) Hydrothermal preparation of ZnO electrodes synthesized from different precursors for electrochemical supercapacitors. Synth Met 211:30–34
39. Selvarajan S, Suganthi A, Rajarajan M (2018) A facile synthesis of ZnO/Manganese hexacyanoferrate nanocomposite modified electrode for the electrocatalytic sensing of riboflavin. J Phys Chem Solids 121:350–359
40. Dong G, Du B, Liu L, Zhang W, Liang Y, Shi H, Wang W (2017) Synthesis and their enhanced photoelectrochemical performance of ZnO nanoparticle-loaded CuO dandelion heterostructures under solar light. Appl Surf Sci 399:86–94
41. Duan X, Zhao C, Liu W, Zhao X, Chang L (2017) Fabrication of a novel PbO_2 electrode with a graphene nanosheet interlayer for electrochemical oxidation of 2-chlorophenol. Electrochim Acta 240:424–436
42. Li X, Xu H, Yan W (2016) Fabrication and characterization of PbO_2 electrode modified with polyvinylidene fluoride (PVDF). Appl Surf Sci 389:278–286
43. Amiri-Aref M, Raoof JB, Ojani R (2013) Electrocatalytic oxidation and selective determination of an opioid analgesic methadone in the presence of acetaminophen at a glassy carbon electrode modified with functionalized multi-walled carbon nanotubes: application for human urine, saliva and pharmaceutical samples analysis. Colloids Surf B 109:287–293
44. Chianeh FN, Parsa JB (2014) Degradation of azo dye from aqueous solutions using nano-SnO_2/Ti electrode prepared by electrophoretic deposition method: experimental design. Chem Eng Res Des 92(11):2740–2748
45. Croissant M, Napporn T, Léger J-M, Lamy C (1998) Electrocatalytic oxidation of hydrogen at platinum-modified polyaniline electrodes. Electrochim Acta 43(16–17):2447–2457
46. Raoof J-B, Ojani R, Rashid-Nadimi S (2004) Preparation of polypyrrole/ferrocyanide films modified carbon paste electrode and its application on the electrocatalytic determination of ascorbic acid. Electrochim Acta 49(2):271–280
47. Tashkhourian J, Hemmateenejad B, Beigizadeh H, Hosseini-Sarvari M, Razmi Z (2014) ZnO nanoparticles and multiwalled carbon nanotubes modified carbon paste electrode for determination of naproxen using electrochemical techniques. J Electroanal Chem 714:103–108
48. Zhang L, Xu L, He J, Zhang J (2014) Preparation of Ti/SnO_2–Sb electrodes modified by carbon nanotube for anodic oxidation of dye wastewater and combination with nanofiltration. Electrochim Acta 117:192–201
49. Esmaelian M, Chianeh FN, Asghari A (2019) Degradation of ciprofloxacin using electrochemical oxidation by Ti/nanoSnO_2–MWCNT electrode: optimization and modelling through central composite design. J Ind Eng Chem 78:97–105
50. Amani-Beni Z, Nezamzadeh-Ejhieh A (2017) A novel non-enzymatic glucose sensor based on the modification of carbon paste electrode with CuO nanoflower: designing the experiments by response surface methodology (RSM). J Colloid Interface Sci 504:186–196
51. Güven G, Perendeci A, Tanyolaç A (2008) Electrochemical treatment of deproteinated whey wastewater and optimization of treatment conditions with response surface methodology. J Hazard Mater 157(1):69–78
52. Shoorangiz M, Nikoo MR, Salari M, Rakhshandehroo GR, Sadegh M (2019) Optimized electro-Fenton process with sacrificial stainless steel anode for degradation/mineralization of ciprofloxacin. Process Saf Environ Prot 132:340–350
53. Ansari MH, Parsa JB, Merati Z (2017) Removal of fluoride from water by nanocomposites of POPOA/Fe_3O_4, POPOA/TiO_2, POPOT/Fe_3O_4 and POPOT/TiO_2: modelling and optimization via RSM. Chem Eng Res Des 126:1–18
54. Li X, Xu H, Yan W (2016) Electrochemical oxidation of aniline by a novel Ti/TiOxHy/Sb–SnO_2 electrode. Chin J Catal 37(11):1860–1870
55. Alaoui A, El Kacemi K, El Ass K, Kitane S, El Bouzidi S (2015) Activity of Pt/MnO_2 electrode in the electrochemical degradation of methylene blue in aqueous solution. Sep Purif Technol 154:281–289
56. Zhou X, Liu S, Yu H, Xu A, Li J, Sun X, Shen J, Han W, Wang L (2018) Electrochemical oxidation of pyrrole, pyrazole and tetrazole using a TiO_2 nanotubes based SnO_2–Sb/3D highly ordered macro-porous PbO_2 electrode. J Electroanal Chem 826:181–190
57. Kaur R, Kushwaha JP, Singh N (2019) Amoxicillin electro-catalytic oxidation using Ti/RuO_2 anode: mechanism, oxidation products and degradation pathway. Electrochim Acta 296:856–866
58. Sandhwar VK, Prasad B (2019) A comparative study of electrochemical degradation of benzoic acid and terephthalic acid from aqueous solution of purified terephthalic acid (PTA) wastewater. J Water Process Eng 30:100381
59. Martinez-Huitle CA, Ferro S (2006) Electrochemical oxidation of organic pollutants for the wastewater treatment: direct and indirect processes. Chem Soc Rev 35(12):1324–1340
60. Wan J, Liu B, Jin C, Li J, Wei X, Dong H, Xu Z, Gao M, Zhao Y (2019) Electrochemical oxidation of Acid Black 2 dye wastewater using boron-doped diamond anodes: multiresponse optimization and degradation mechanisms. Environ Eng Sci 36(9):1049–1060
61. Martínez-Huitle CA, Rodrigo MA, Sires I, Scialdone O (2015) Single and coupled electrochemical processes and reactors for the abatement of organic water pollutants: a critical review. Chem Rev 115(24):13362–13407
62. Chianeh FN, Avestan MS (2020) Application of central composite design for electrochemical oxidation of reactive dye on Ti/MWCNT electrode. J Iran Chem Soc 17(5):1073–1085
63. Singh N, Routara B, Das D (2018) Study of machining characteristics of Inconel 601in EDM using RSM. Mater Today Proc 5(2):3438–3449
64. Aquino JM, Rocha-Filho RC, Bocchi N, Biaggio SR (2013) Electrochemical degradation of the Disperse Orange 29 dye on a β-PbO_2 anode assessed by the response surface methodology. J Environ Chem Eng 1(4):954–961
65. Yao Y, Zhao M, Zhao C, Zhang H (2014) Preparation and properties of PbO_2–ZrO_2 nanocomposite electrodes by pulse electrodeposition. Electrochim Acta 117:453–459